

Measurement of $D^0\text{-}\bar{D}^0$ mixing in $D^0 \rightarrow K_S^0 \pi^+ \pi^-$ decays

L. M. Zhang,³⁷ Z. P. Zhang,³⁷ I. Adachi,⁷ H. Aihara,⁴⁵ V. Aulchenko,¹ T. Aushev,^{18,13} A. M. Bakich,⁴⁰ V. Balagura,¹³ E. Barberio,²¹ A. Bay,¹⁸ K. Belous,¹² U. Bitenc,¹⁴ A. Bondar,¹ A. Bozek,²⁷ M. Bračko,^{20,14} J. Brodzicka,⁷ T. E. Browder,⁶ P. Chang,²⁶ Y. Chao,²⁶ A. Chen,²⁴ K.-F. Chen,²⁶ W. T. Chen,²⁴ B. G. Cheon,⁵ C.-C. Chiang,²⁶ I.-S. Cho,⁵⁰ Y. Choi,³⁹ Y. K. Choi,³⁹ J. Dalseno,²¹ M. Danilov,¹³ M. Dash,⁴⁹ A. Drutskoy,³ S. Eidelman,¹ D. Epifanov,¹ S. Fratina,¹⁴ N. Gabyshev,¹ G. Gokhroo,⁴¹ B. Golob,^{19,14} H. Ha,¹⁶ J. Haba,⁷ T. Hara,³² N. C. Hastings,⁴⁵ K. Hayasaka,²² H. Hayashii,²³ M. Hazumi,⁷ D. Heffernan,³² T. Hokuue,²² Y. Hoshi,⁴³ W.-S. Hou,²⁶ Y. B. Hsiung,²⁶ H. J. Hyun,¹⁷ T. Iijima,²² K. Ikado,²² K. Inami,²² A. Ishikawa,⁴⁵ H. Ishino,⁴⁶ R. Itoh,⁷ M. Iwasaki,⁴⁵ Y. Iwasaki,⁷ N. J. Joshi,⁴¹ D. H. Kah,¹⁷ H. Kaji,²² S. Kajiwara,³² J. H. Kang,⁵⁰ H. Kawai,² T. Kawasaki,²⁹ H. Kichimi,⁷ H. J. Kim,¹⁷ H. O. Kim,³⁹ S. K. Kim,³⁸ Y. J. Kim,⁴ K. Kinoshita,³ S. Korpar,^{20,14} P. Krizán,^{19,14} P. Krokovny,⁷ R. Kumar,³³ C. C. Kuo,²⁴ A. Kuzmin,¹ Y.-J. Kwon,⁵⁰ J. S. Lee,³⁹ M. J. Lee,³⁸ S. E. Lee,³⁸ T. Lesiak,²⁷ J. Li,⁶ A. Limosani,²¹ S.-W. Lin,²⁶ Y. Liu,⁴ D. Liventsev,¹³ T. Matsumoto,⁴⁷ A. Matyja,²⁷ S. McOnie,⁴⁰ T. Medvedeva,¹³ W. Mitaroff,¹¹ H. Miyake,³² H. Miyata,²⁹ Y. Miyazaki,²² R. Mizuk,¹³ Y. Nagasaka,⁸ I. Nakamura,⁷ E. Nakano,³¹ M. Nakao,⁷ Z. Natkaniec,²⁷ S. Nishida,⁷ O. Nitoh,⁴⁸ S. Ogawa,⁴² T. Ohshima,²² S. Okuno,¹⁵ S. L. Olsen,⁶ Y. Onuki,³⁵ W. Ostrowicz,²⁷ H. Ozaki,⁷ P. Pakhlov,¹³ G. Pakhlova,¹³ C. W. Park,³⁹ H. Park,¹⁷ L. S. Peak,⁴⁰ R. Pestotnik,¹⁴ L. E. Piilonen,⁴⁹ A. Poluektov,¹ H. Sahoo,⁶ Y. Sakai,⁷ O. Schneider,¹⁸ J. Schümann,⁷ C. Schwanda,¹¹ A. J. Schwartz,³ R. Seidl,^{9,35} K. Senyo,²² M. E. Sevier,²¹ M. Shapkin,¹² H. Shibuya,⁴² S. Shinomiya,³² J.-G. Shiu,²⁶ B. Shwartz,¹ J. B. Singh,³³ A. Sokolov,¹² A. Somov,³ N. Soni,³³ S. Stanič,³⁰ M. Starič,¹⁴ H. Stoeck,⁴⁰ K. Sumisawa,⁷ T. Sumiyoshi,⁴⁷ S. Suzuki,³⁶ O. Tajima,⁷ F. Takasaki,⁷ K. Tamai,⁷ N. Tamura,²⁹ M. Tanaka,⁷ G. N. Taylor,²¹ Y. Teramoto,³¹ X. C. Tian,³⁴ I. Tikhomirov,¹³ T. Tsuboyama,⁷ S. Uehara,⁷ K. Ueno,²⁶ T. Uglov,¹³ Y. Unno,⁵ S. Uno,⁷ P. Urquijo,²¹ Y. Usov,¹ G. Varner,⁶ K. Vervink,¹⁸ S. Villa,¹⁸ A. Vinokurova,¹ C. H. Wang,²⁵ M.-Z. Wang,²⁶ P. Wang,¹⁰ Y. Watanabe,¹⁵ E. Won,¹⁶ B. D. Yabsley,⁴⁰ A. Yamaguchi,⁴⁴ Y. Yamashita,²⁸ M. Yamauchi,⁷ C. Z. Yuan,¹⁰ C. C. Zhang,¹⁰ V. Zhilich,¹ and A. Zupanc¹⁴

(The Belle Collaboration)

¹*Budker Institute of Nuclear Physics, Novosibirsk*

²*Chiba University, Chiba*

³*University of Cincinnati, Cincinnati, Ohio 45221*

⁴*The Graduate University for Advanced Studies, Hayama*

⁵*Hanyang University, Seoul*

⁶*University of Hawaii, Honolulu, Hawaii 96822*

⁷*High Energy Accelerator Research Organization (KEK), Tsukuba*

⁸*Hiroshima Institute of Technology, Hiroshima*

⁹*University of Illinois at Urbana-Champaign, Urbana, Illinois 61801*

¹⁰*Institute of High Energy Physics, Chinese Academy of Sciences, Beijing*

¹¹*Institute of High Energy Physics, Vienna*

¹²*Institute of High Energy Physics, Protvino*

¹³*Institute for Theoretical and Experimental Physics, Moscow*

¹⁴*J. Stefan Institute, Ljubljana*

¹⁵*Kanagawa University, Yokohama*

¹⁶*Korea University, Seoul*

¹⁷*Kyungpook National University, Taegu*

¹⁸*Swiss Federal Institute of Technology of Lausanne, EPFL, Lausanne*

¹⁹*University of Ljubljana, Ljubljana*

²⁰*University of Maribor, Maribor*

²¹*University of Melbourne, School of Physics, Victoria 3010*

²²*Nagoya University, Nagoya*

²³*Nara Women's University, Nara*

²⁴*National Central University, Chung-li*

²⁵*National United University, Miao Li*

²⁶*Department of Physics, National Taiwan University, Taipei*

²⁷*H. Niewodniczanski Institute of Nuclear Physics, Krakow*

²⁸*Nippon Dental University, Niigata*

²⁹*Niigata University, Niigata*

³⁰*University of Nova Gorica, Nova Gorica*

³¹*Osaka City University, Osaka*

³²*Osaka University, Osaka*

³³Panjab University, Chandigarh³⁴Peking University, Beijing³⁵RIKEN BNL Research Center, Upton, New York 11973³⁶Saga University, Saga³⁷University of Science and Technology of China, Hefei³⁸Seoul National University, Seoul³⁹Sungkyunkwan University, Suwon⁴⁰University of Sydney, Sydney, New South Wales⁴¹Tata Institute of Fundamental Research, Mumbai⁴²Toho University, Funabashi⁴³Tohoku Gakuin University, Tagajo⁴⁴Tohoku University, Sendai⁴⁵Department of Physics, University of Tokyo, Tokyo⁴⁶Tokyo Institute of Technology, Tokyo⁴⁷Tokyo Metropolitan University, Tokyo⁴⁸Tokyo University of Agriculture and Technology, Tokyo⁴⁹Virginia Polytechnic Institute and State University, Blacksburg, Virginia 24061⁵⁰Yonsei University, Seoul

We report a measurement of D^0 - \bar{D}^0 mixing in $D^0 \rightarrow K_S^0 \pi^+ \pi^-$ decays using a time-dependent Dalitz plot analysis. We first assume CP conservation and subsequently allow for CP violation. The results are based on 540 fb^{-1} of data accumulated with the Belle detector at the KEKB e^+e^- collider. Assuming negligible CP violation, we measure the mixing parameters $x = (0.80 \pm 0.29_{-0.07}^{+0.09} + 0.10_{-0.14}^{+0.10})\%$ and $y = (0.33 \pm 0.24_{-0.12}^{+0.08} + 0.06_{-0.08}^{+0.06})\%$, where the errors are statistical, experimental systematic, and systematic due to the Dalitz decay model, respectively. Allowing for CP violation, we obtain the CPV parameters $|q/p| = 0.86_{-0.29}^{+0.30} + 0.06_{-0.03}^{+0.06} \pm 0.08$ and $\arg(q/p) = (-14_{-18}^{+16} + 5_{-3}^{+2})^\circ$.

PACS numbers: 13.25.Ft, 11.30.Er, 12.15.Ff

Mixing in the D^0 - \bar{D}^0 system is predicted to be very small in the Standard Model (SM) [1] and, unlike in K^0 , B^0 , and B_s^0 systems, has eluded experimental observation. Recently, evidence for this phenomenon has been found in $D^0 \rightarrow K^+ K^- / \pi^+ \pi^-$ [2] and $D^0 \rightarrow K^+ \pi^-$ [3] decays. It is important to measure D^0 - \bar{D}^0 mixing in other decay modes and to search for CP -violating (CPV) effects in order to determine whether physics contributions outside the SM are present. Here we study the self-conjugate decay $D^0 \rightarrow K_S^0 \pi^+ \pi^-$.

The time-dependent probability of flavor eigenstates D^0 and \bar{D}^0 to mix to each other is governed by the lifetime $\tau_{D^0} = 1/\Gamma$, and the mixing parameters $x = (m_1 - m_2)/\Gamma$ and $y = (\Gamma_1 - \Gamma_2)/2\Gamma$. The parameters m_1, m_2 (Γ_1, Γ_2) are the masses (decay widths) of the mass eigenstates $|D_{1,2}\rangle = p|D^0\rangle \pm q|\bar{D}^0\rangle$, and $\Gamma = (\Gamma_1 + \Gamma_2)/2$. The parameters p and q are complex coefficients satisfying $|p|^2 + |q|^2 = 1$. Various D^0 decay modes have been exploited to measure or constrain x and y [4]. For $D^0 \rightarrow K_S^0 \pi^+ \pi^-$ decays, the time dependence of the Dalitz plot distribution allows one to measure x and y directly. This method was developed by CLEO [5] using 9.0 fb^{-1} of data; here we extend this method to a data sample 60 times larger.

The decay amplitude at time t of an initially produced $|D^0\rangle$ or $|\bar{D}^0\rangle$ can be expressed as

$$\mathcal{M}(m_-^2, m_+^2, t) = \mathcal{A}(m_-^2, m_+^2) \frac{e_1(t) + e_2(t)}{2}$$

$$\begin{aligned} & + \frac{q}{p} \bar{\mathcal{A}}(m_-^2, m_+^2) \frac{e_1(t) - e_2(t)}{2}, \\ \bar{\mathcal{M}}(m_-^2, m_+^2, t) & = \bar{\mathcal{A}}(m_-^2, m_+^2) \frac{e_1(t) + e_2(t)}{2} \\ & + \frac{p}{q} \mathcal{A}(m_-^2, m_+^2) \frac{e_1(t) - e_2(t)}{2}, \end{aligned} \quad (1)$$

where \mathcal{A} and $\bar{\mathcal{A}}$ are the amplitudes for $|D^0\rangle$ and $|\bar{D}^0\rangle$ decays as functions of the invariant-masses-squared variables $m_\pm^2 \equiv m^2(K_S^0 \pi^\pm)$. The time dependence is contained in the terms $e_{1,2}(t) = \exp[-i(m_{1,2} - i\Gamma_{1,2}/2)t]$. Upon squaring \mathcal{M} and $\bar{\mathcal{M}}$, one obtains decay rates containing terms $\exp(-\Gamma t) \cos(x\Gamma t)$, $\exp(-\Gamma t) \sin(x\Gamma t)$, and $\exp[-(1 \pm y)\Gamma t]$.

We parameterize the $K_S^0 \pi^+ \pi^-$ Dalitz distribution following Ref. [6]. The overall amplitude as a function of m_+^2 and m_-^2 is expressed as a sum of quasi-two-body amplitudes (subscript r) and a constant non-resonant term (subscript NR):

$$\mathcal{A}(m_-^2, m_+^2) = \sum_r a_r e^{i\phi_r} \mathcal{A}_r(m_-^2, m_+^2) + a_{\text{NR}} e^{i\phi_{\text{NR}}}, \quad (2)$$

$$\bar{\mathcal{A}}(m_-^2, m_+^2) = \sum_r \bar{a}_r e^{i\bar{\phi}_r} \mathcal{A}_r(m_+^2, m_-^2) + \bar{a}_{\text{NR}} e^{i\bar{\phi}_{\text{NR}}}. \quad (3)$$

The functions \mathcal{A}_r are products of Blatt-Weisskopf form factors and relativistic Breit-Wigner functions [7].

The data were recorded by the Belle detector at the KEKB asymmetric-energy e^+e^- collider [8]. The Belle detector [9] includes a silicon vertex detector (SVD), a

central drift chamber (CDC), an array of aerogel threshold Cherenkov counters (ACC), a barrel-like arrangement of time-of-flight scintillation counters (TOF), and an electromagnetic calorimeter.

We reconstruct D^0 candidates via the decay chain $D^{*+} \rightarrow \pi_s^+ D^0$, $D^0 \rightarrow K_S^0 \pi^+ \pi^-$ [10]. Here, π_s denotes a low-momentum pion, the charge of which tags the flavor of the neutral D at production. The K_S^0 candidates are reconstructed in the $\pi^+ \pi^-$ final state; we require that the pion candidates form a common vertex separated from the interaction region and have an invariant mass within ± 10 MeV/ c^2 of $m_{K_S^0}$. We reconstruct D^0 candidates by combining the K_S^0 candidate with two oppositely charged tracks assigned as pions. These tracks are required to have at least two SVD hits in both r - ϕ and z coordinates. A D^{*+} candidate is reconstructed by combining the D^0 candidate with a low momentum charged track (the π_s^+ candidate); the resulting D^{*+} momentum in the e^+e^- center-of-mass (CM) frame is required to be larger than 2.5 GeV/ c in order to eliminate $B\bar{B}$ events and suppress combinatorial background.

The charged pion tracks are refitted to originate from a common vertex, which represents the decay point of the D^0 . The D^{*+} vertex is taken to be the intersection of the D^0 momentum vector with the e^+e^- interaction region. The D^0 proper decay time is calculated from the projection of the vector joining the two vertices (\vec{L}) onto the momentum vector: $t = \vec{L} \cdot (\vec{p}/p)(m_{D^0}/p)$. The uncertainty in t (σ_t) is calculated event-by-event, and we require $\sigma_t < 1$ ps (for selected events, $\langle \sigma_t \rangle \sim 0.2$ ps).

The signal and background yields are determined from a two-dimensional fit to the variables $m_{K_S^0 \pi \pi}$ and $Q \equiv (m_{K_S^0 \pi \pi} - m_{K_S^0 \pi \pi} - m_{\pi}) \cdot c^2$. The variable Q is the kinetic energy released in the decay and equals only 5.9 MeV for $D^{*+} \rightarrow \pi_s^+ D^0$ decays. We parameterize the signal shape by a triple-Gaussian function for $m_{K_S^0 \pi \pi}$, and the sum of a bifurcated Student t distribution and a Gaussian function for Q . The backgrounds are classified into two types: random π_s background, in which a random π_s is combined with a true D^0 decay, and combinatorial background. The shape of the $m_{K_S^0 \pi \pi}$ distribution for the random π_s background is fixed to be the same as that used for the signal. Other background distributions are obtained from Monte Carlo (MC) simulation. We perform a two-dimensional fit to the measured $m_{K_S^0 \pi \pi}$ - Q distributions in a wide range 1.81 GeV/ $c^2 < m_{K_S^0 \pi \pi} < 1.92$ GeV/ c^2 and $0 < Q < 20$ MeV. We define a smaller signal region $|m_{K_S^0 \pi \pi} - m_{D^0}| < 15$ MeV/ c^2 and $|Q - 5.9$ MeV| < 1.0 MeV, corresponding to 3σ intervals in these variables. In this region we find 534410 ± 830 signal events and background fractions of 1% and 4% for the random π_s and combinatorial backgrounds, respectively. The $m_{K_S^0 \pi \pi}$ and Q distributions are shown in Fig. 1 along

with projections of the fit result.

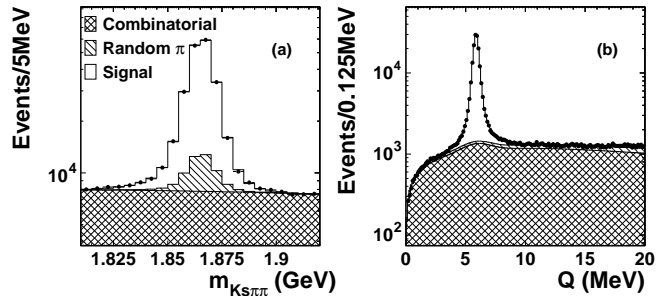


FIG. 1: The distribution of (a) $m_{K_S^0 \pi \pi}$ with $0 < Q < 20$ MeV; (b) Q with 1.81 GeV/ $c^2 < m_{K_S^0 \pi \pi} < 1.92$ GeV/ c^2 . Superimposed on the data (points with error bars) are projections of the $m_{K_S^0 \pi \pi}$ - Q fit.

For the events selected in the signal region we perform an unbinned likelihood fit to the Dalitz plot variables m_-^2 and m_+^2 , and the decay time t . For D^0 decays, the likelihood function is

$$\mathcal{L} = \prod_{i=1}^{N_{D^0}} \sum_j f_j(m_{K_S^0 \pi \pi, i}, Q_i) \mathcal{P}_j(m_-^2, m_+^2, t_i), \quad (4)$$

where $j = \{\text{sig, rnd, cmb}\}$ denotes the signal or background components, and the index i runs over D^0 candidates. The event weights f_j are functions of $m_{K_S^0 \pi \pi}$ and Q and are obtained from the $m_{K_S^0 \pi \pi}$ - Q fit mentioned above.

The probability density function (PDF) $\mathcal{P}_{\text{sig}}(m_-^2, m_+^2, t)$ equals $|\mathcal{M}(m_-^2, m_+^2, t)|^2$ convolved with the detector response. Resolution effects in two-particle invariant masses are significant only for $m_{\pi \pi}^2$. The latter, and variation of the efficiency across the Dalitz plot, are taken into account using the method described in Ref. [6]. The resolution in decay time t is accounted for by convolving \mathcal{P}_{sig} with a resolution function consisting of a sum of three Gaussians with a common mean and widths $\sigma_k = S_k \cdot \sigma_{t, i}$ ($k = 1-3$). The scale factors S_k and the common mean are free parameters in the fit.

The random π_s background contains real D^0 and \bar{D}^0 decays; in this case the charge of the π_s is uncorrelated with the flavor of the neutral D . Thus the \mathcal{P}_{rnd} PDF is taken to be $(1 - f_w)|\mathcal{M}(m_-^2, m_+^2, t)|^2 + f_w|\overline{\mathcal{M}}(m_-^2, m_+^2, t)|^2$, convolved with the same resolution function as that used for the signal, where f_w is the wrong-tag fraction. We measure $f_w = 0.452 \pm 0.005$ from fitting events in the Q sideband 3 MeV $< |Q - 5.9$ MeV| < 14.1 MeV.

For the combinatorial background, \mathcal{P}_{cmb} is the product of Dalitz-plot and decay time PDFs. The latter is parameterized as the sum of a delta function and an

exponential function convolved with a Gaussian resolution function. The timing and Dalitz PDF parameters are obtained from fitting events in the mass sideband $30 \text{ MeV}/c^2 < |m_{K_S^0 \pi \pi} - m_{D^0}| < 55 \text{ MeV}/c^2$.

The likelihood function for \overline{D}^0 decays, $\overline{\mathcal{L}}$, has the same form as \mathcal{L} , with \mathcal{M} and $\overline{\mathcal{M}}$ (appearing in \mathcal{P}_{sig} and \mathcal{P}_{rnd}) interchanged. To determine x and y , we maximize the sum $\ln \mathcal{L} + \ln \overline{\mathcal{L}}$. Table I lists the results from two separate fits. In the first fit we assume CP is conserved, i.e., $a = \bar{a}$, $\phi = \bar{\phi}$, and $p/q = 1$. We fit all events in the signal region, where the free parameters are x , y , τ_{D^0} , the timing resolution parameters of the signal, and the Dalitz plot resonance parameters $a_r(\text{NR})$ and $\phi_r(\text{NR})$. The fit gives $\tau_{D^0} = (409.9 \pm 1.0)$ fs, which is consistent with the world average [11]. The results for a_r and ϕ_r for the 18 quasi-two-body resonances used (following the same model as in Ref. [6]) and the NR contribution are listed in Table II. The Dalitz plot and its projections, along with projections of the fit result, are shown in Fig. 2. We estimate the goodness-of-fit of the Dalitz plot through a two-dimensional χ^2 test [6] and obtain $\chi^2/\text{ndf} = 2.1$ for $3653 - 40$ degrees of freedom (ndf). We find that the main features of the Dalitz plot are well reproduced, with some significant but numerically small discrepancies at peaks and dips of the distribution in the very high m_-^2 region. The decay-time distribution for all events, and the ratio of decay-time distribution for events in the $K^*(892)^+$ and $K^*(892)^-$ regions, are shown in Fig. 3.

TABLE I: Fit results and 95% C.L. intervals for x and y , including systematic uncertainties. The errors are statistical, experimental systematic, and decay-model systematic, respectively. For the CPV -allowed case, there is another solution as described in the text.

Fit case	Parameter	Fit result	95% C.L. interval
No	$x(\%)$	$0.80 \pm 0.29^{+0.09+0.10}_{-0.07-0.14}$	(0.0, 1.6)
CPV	$y(\%)$	$0.33 \pm 0.24^{+0.08+0.06}_{-0.12-0.08}$	(-0.34, 0.96)
CPV	$x(\%)$	$0.81 \pm 0.30^{+0.10+0.09}_{-0.07-0.16}$	$ x < 1.6$
	$y(\%)$	$0.37 \pm 0.25^{+0.07+0.07}_{-0.13-0.08}$	$ y < 1.04$
	$ q/p $	$0.86^{+0.30+0.06}_{-0.29-0.03} \pm 0.08$	-
	$\arg(q/p)(^\circ)$	$-14^{+16+5+2}_{-18-3-4}$	-

For the second fit, we allow for CPV . This introduces the additional free parameters $|p/q|$, $\arg(p/q)$, $\bar{a}_r(\text{NR})$ and $\bar{\phi}_r(\text{NR})$. The fit gives two solutions: if $\{x, y, \arg(p/q)\}$ is a solution, then $\{-x, -y, \arg(p/q) + \pi\}$ is an equally good solution. From the fit to data, we find that the Dalitz plot parameters are consistent for the D^0 and \overline{D}^0 samples; hence we observe no evidence for direct CPV . Results for $|p/q|$ and $\arg(p/q)$, parameterizing CPV in mixing and interference between mixed and unmixed amplitudes, respectively, are also found to be consistent with CP conservation. If we fit the data assuming no direct CPV , the values for x and y are essentially the same as those for the

TABLE II: Fit results for Dalitz plot parameters. The errors are statistical only.

Resonance	Amplitude	Phase ($^\circ$)	Fit fraction
$K^*(892)^-$	1.629 ± 0.006	134.3 ± 0.3	0.6227
$K_0^*(1430)^-$	2.12 ± 0.02	-0.9 ± 0.8	0.0724
$K_2^*(1430)^-$	0.87 ± 0.02	-47.3 ± 1.2	0.0133
$K^*(1410)^-$	0.65 ± 0.03	111 ± 4	0.0048
$K^*(1680)^-$	0.60 ± 0.25	147 ± 29	0.0002
$K^*(892)^+$	0.152 ± 0.003	-37.5 ± 1.3	0.0054
$K_0^*(1430)^+$	0.541 ± 0.019	91.8 ± 2.1	0.0047
$K_2^*(1430)^+$	0.276 ± 0.013	-106 ± 3	0.0013
$K^*(1410)^+$	0.33 ± 0.02	-102 ± 4	0.0013
$K^*(1680)^+$	0.73 ± 0.16	103 ± 11	0.0004
$\rho(770)$	1 (fixed)	0 (fixed)	0.2111
$\omega(782)$	0.0380 ± 0.0007	115.1 ± 1.1	0.0063
$f_0(980)$	0.380 ± 0.004	-147.1 ± 1.1	0.0452
$f_0(1370)$	1.46 ± 0.05	98.6 ± 1.8	0.0162
$f_2(1270)$	1.43 ± 0.02	-13.6 ± 1.2	0.0180
$\rho(1450)$	0.72 ± 0.04	41 ± 7	0.0024
σ_1	1.39 ± 0.02	-146.6 ± 0.9	0.0914
σ_2	0.267 ± 0.013	-157 ± 3	0.0088
NR	2.36 ± 0.07	155 ± 2	0.0615

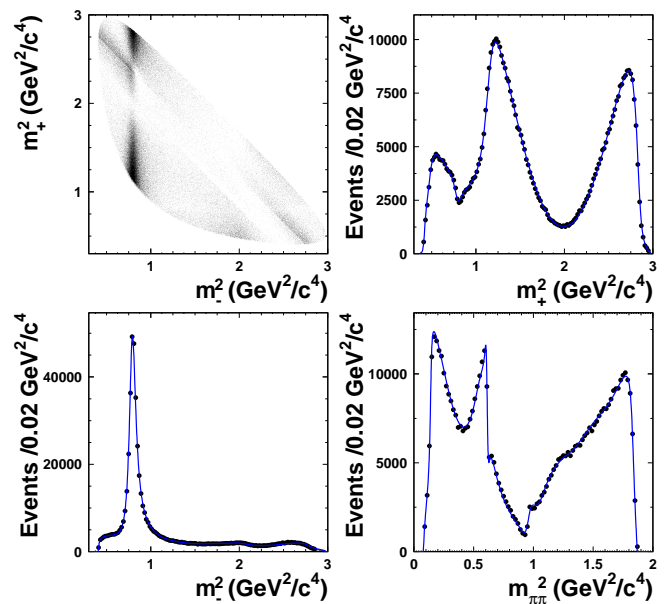


FIG. 2: Dalitz plot distribution and the projections for data (points with error bars) and the fit result (curve). Here, m_{\pm}^2 corresponds to $m^2(K_S^0 \pi^{\pm})$ for D^0 decays and to $m^2(K_S^0 \pi^{\mp})$ for \overline{D}^0 decays.

CP -conservation case, and the values for the CPV parameters are further constrained: $|q/p| = 0.95^{+0.22}_{-0.20}$ and $\arg(q/p) = (-2^{+10}_{-11})^\circ$. A check with independent fits to the D^0 and \overline{D}^0 tagged samples gives consistent results for x (y): $0.58\% \pm 0.41\%$ ($0.45\% \pm 0.33\%$) and $1.04\% \pm 0.41\%$ ($0.21\% \pm 0.34\%$), respectively.

We consider systematic uncertainties arising from both experimental sources and from the $D^0 \rightarrow K_S^0 \pi^+ \pi^-$ decay

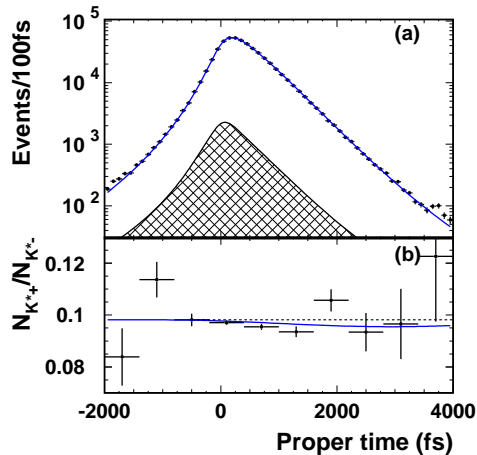


FIG. 3: (a) The decay-time distribution for events in the Dalitz plot fit region for data (points with error bars), and the fit projection for the CP -conservation fit (curve). The hatched area represents the combinatorial background contribution. (b) Ratio of decay-time distributions for events in the $K^*(892)^+$ and $K^*(892)^-$ regions.

model. We estimate these uncertainties by varying relevant parameters by their $\pm 1\sigma$ errors and interpreting the change in x and y as the systematic uncertainty due to that source. The main sources of experimental uncertainty are the modeling of the background, the efficiency, and the event selection criteria. We vary the background normalization and timing parameters within their uncertainties, and we also set f_w equal to its expected value of 0.5 or alternatively let it float. To investigate possible correlations between the Dalitz plot (m_+^2, m_-^2) distribution and the t distribution of combinatorial background, the Dalitz plot distribution is obtained for three bins of decay time; these PDFs are then used according to the reconstructed t of individual events. We also try a uniform efficiency function, and we apply a “best-candidate” selection to check the effect of the small fraction of multiple-candidate events. We add all variations in x and y in quadrature to obtain the overall experimental systematic error.

The systematic error due to our choice of $D^0 \rightarrow K_S^0 \pi^+ \pi^-$ decay model is evaluated as follows. We vary the masses and widths of the intermediate resonances by their known uncertainties [11], and we also try fits with Blatt-Weisskopf form factors set to unity and with no q^2 dependence in the Breit-Wigner widths. We perform a series of fits successively excluding intermediate resonances that give small contributions ($\rho(1450)$, $K^*(1680)^+$), and we also exclude the NR contribution. We account for uncertainty in modeling of the S -wave $\pi\pi$ component by using K-matrix formalism [12]. We include an uncertainty due to the effect of around 10-20% bias in the amplitudes for the $K^*(1410)^\pm$, $K_0^*(1430)^+$ and $K_2^*(1430)^+$ intermediate states, which we

observe in MC studies. Adding all variations in quadrature gives the final results listed in Table I.

We obtain a 95% C.L. contour in the (x, y) plane by finding the locus of points where $-2\ln\mathcal{L}$ increases by 5.99 units with respect to the minimum value (i.e., $-2\Delta\ln\mathcal{L}=5.99$). All fit variables other than x and y are allowed to vary to obtain best-fit values at each point on the contour. To include systematic uncertainty, we rescale each point on the contour by a factor $\sqrt{1+r^2}$, where r^2 is a weighted average of the ratios of systematic to statistical errors for x and y , where the weights depend on the position on the contour. Both the statistical-only and overall contours for both the CPV -allowed and the CP -conservation case are shown in Fig. 4. We note that for the CPV -allowed case, the reflection of these contours through the origin $(0,0)$ are also allowed regions. Projecting the overall contour onto the x, y axes gives the 95% C.L. intervals listed in Table I. After the systematics-rescaling procedure, the no-mixing point $(0,0)$ has a value $-2\Delta\ln\mathcal{L} = 7.3$; this corresponds to a C.L. of 2.6%. We have confirmed this value by generating and fitting an ensemble of MC fast-simulated experiments.

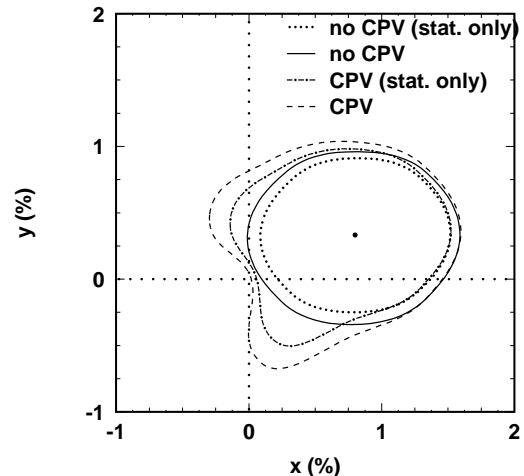


FIG. 4: 95% C.L. contours for (x, y) : dotted (solid) corresponds to statistical (statistical and systematic) contour for no CPV , and dash-dotted (dashed) corresponds to statistical (statistical and systematic) contour for the CPV -allowed case. The point is the best-fit result for no CPV .

In summary, we have measured the $D^0-\bar{D}^0$ mixing parameters x and y using a Dalitz plot analysis of $D^0 \rightarrow K_S^0 \pi^+ \pi^-$ decays. Assuming negligible CP violation, we measure $x = (0.80 \pm 0.29_{-0.07}^{+0.09+0.10})\%$ and $y = (0.33 \pm 0.24_{-0.12}^{+0.08+0.06})\%$, where the errors are statistical, experimental systematic, and decay-model systematic, respectively. Our results disfavor the no-mixing point $x = y = 0$ with a significance of 2.2σ , while the one dimensional significance for $x > 0$ is 2.4σ . We have also searched for CPV ; we see no evidence for this and

constrain the CPV parameters $|q/p|$ and $\arg(q/p)$.

We thank the KEKB group for excellent operation of the accelerator, the KEK cryogenics group for efficient solenoid operations, and the KEK computer group and the NII for valuable computing and Super-SINET network support. We acknowledge support from MEXT and JSPS (Japan); ARC and DEST (Australia); NSFC and KIP of CAS (China); DST (India); MOEHRD, KOSEF and KRF (Korea); KBN (Poland); MES and RFAAE (Russia); ARRS (Slovenia); SNSF (Switzerland); NSC and MOE (Taiwan); and DOE (USA).

-
- [1] A. F. Falk *et al.*, Phys. Rev. D **65**, 054034 (2002); I. I. Bigi, N. Uraltsev, Nucl. Phys. B **592**, 92 (2001); A. F. Falk *et al.*, Phys. Rev. D **69**, 114021 (2004); A. A. Petrov, Int. J. Mod. Phys. A **21**, 5686 (2006).
- [2] M. Starič *et al.* (Belle Collaboration), Phys. Rev. Lett. **98**, 211803 (2007).
- [3] B. Aubert *et al.* (BaBar Collaboration), Phys. Rev. Lett. **98**, 211802 (2007).
- [4] For a review see: D. M. Asner, D^0 - \bar{D}^0 Mixing, in Ref. [11].
- [5] D. M. Asner *et al.* (CLEO Collaboration), Phys. Rev. D **72**, 012001 (2005) and arXiv: hep-ex/0503045v3.
- [6] A. Poluektov *et al.* (Belle Collaboration), Phys. Rev. D **73**, 112009 (2006).
- [7] S. Kopp *et al.* (CLEO Collaboration), Phys. Rev. D **63**, 092001 (2001).
- [8] S. Kurokawa, E. Kikutani *et al.*, Nucl. Instrum. Methods Phys. Res. Sect. A **499**, 1 (2003), and other papers in this volume.
- [9] A. Abashian *et al.* (Belle Collaboration), Nucl. Instrum. Methods Phys. Res. Sect. A **479**, 117 (2002); Z. Natkaniec *et al.* (Belle SVD2 Group), Nucl. Instrum. Methods Phys. Res. Sect. A **560**, 1 (2006).
- [10] Charge conjugate decays are implied unless explicitly stated otherwise.
- [11] W.-M. Yao *et al.* (Particle Data Group), J. Phys. G **33**, 1 (2006).
- [12] J. M. Link *et al.* (FOCUS Collaboration), Phys. Lett. B **585**, 200 (2004); B. Aubert *et al.* (BaBar Collaboration), arXiv: hep-ex/0507101.